Check for updates

Chemistry Europe
European Chemical Societies Publishing

Identification of Photoexcited Electron Relaxation in a Cobalt Phosphide Modified Carbon Nitride Photocatalyst

Guang Xian Pei,[a] Nelson Y. Dzade,[b] Yue Zhang,[c] Jan P. Hofmann,[c, d] Nora H. de Leeuw,[b, e, f] and Bert M. Weckhuysen*[a]

Transition metal phosphides have been recognized as efficient co-catalysts to boost the activity of semiconductor photocatalysts. However, a rigorous and quantitative understanding is still to be developed about how transition metal phosphides influence photoexcited electron dynamics. Here, we present a nanosecond time-resolved transient absorption spectroscopy (TAS) study of the photoexcited electron dynamics in carbon nitrides (g-C_3N_4) before and after Co and/or P modifications. Our spectroscopic study showed that Co or P lowered the initial electron density, whereas they promoted the photoexcited electron relaxation of g-C_3N_4, with their half-life times ($t_{50\%}$) of 2.5 and 1.8 ns, respectively. The formation of a CoP co-catalyst compound promoted the electron relaxation ($t_{50\%}$ = 2.8 ns) without significantly lowering the charge separation efficiency. Density functional theory (DFT) calculations were undertaken to explore the underlying fundamental reasons and they further predicted that CoP, compared to Co or P modification, better facilitates photoexcited electron transfer from g-C_3N_4 to reactants.

Solar-to-fuel conversion is a promising route to store solar energy in a way that compensates for increasing environmental issues caused by fossil fuel consumption.[1] In principle, the formation of electron-hole pairs in photocatalysts upon illumination and their subsequent involvement in redox reactions are the main processes in photocatalytic conversion. To achieve highly efficient photochemical conversion, the main challenge in photocatalysis is to maximize the extraction of charge carriers while suppressing their recombination.[2]

Co-catalyst/semiconductor heterostructures have been the focus of many investigations in recent years for photocatalysis and solar energy conversion. Co-catalysts will not only serve as active sites, but also promote the photo-excited charge separation and transfer,[3] thus enhancing the photocatalytic activity. Significant attention has been drawn to transition metal phosphides (*e.g.*, FeP, CoP, and NiP),[4] because of their low cost, earth abundance and high electrochemical activity. CoP in particular has been extensively studied as an effective co-catalyst for photocatalytic water splitting and CO_2 reduction reactions.[5] The reason for its enhanced O_2 evolution activity has been ascribed to the increased life-time of photogenerated holes.[6] However, its contribution to photogenerated electron dynamics remains elusive, although Co and/or P can significantly enhance the catalytic activity towards H_2 evolution and CO_2 reduction reactions.[5b–d]

Carbon nitride (g-C_3N_4), known as a polymeric semiconductor for H_2 evolution since the 19th century, is attracting significant research interest because of its visible light photocatalytic performance, good physicochemical stability and facile synthesis.[7] However, only a handful of studies have focused on its fundamental photophysical processes, especially the photoexcited electron dynamics, which control its photocatalytic activity.[8] It has been reported that CoP-loaded g-C_3N_4 has demonstrated higher photocatalytic activity for the H_2 evolution reaction than pristine or Co- or P-modified g-C_3N_4,[9] while the photoexcited electron dynamics of Co- and/or P-loaded g-C_3N_4 remain elusive. The current work seeks to uncover Co and/or P effects on the photoexcited electron dynamics in g-C_3N_4 by combining transient absorption spectroscopy (TAS) with density functional theory (DFT) calculations to investigate the structural differences and possible origins for the affected electron relaxation process. This study enables new insights into the fundamental processes that govern electron relaxation dynamics at the transition metal phosphide co-catalyst/semiconductor interface, and therefore provides a unique perspective for the development of low-cost co-catalyst/semiconductor heterostructures for efficient solar-to-fuel conversion.

The experimental investigation was realized by using nanosecond time-resolved pump-probe TAS[10] with a temporal

[a] *Dr. G. X. Pei, Prof. Dr. B. M. Weckhuysen*
Inorganic Chemistry and Catalysis group
Debye Institute for Nanomaterials Science
Utrecht University
Universiteitsweg 99, 3584 CG Utrecht (The Netherlands)
E-mail: b.m.weckhuysen@uu.nl
[b] *Dr. N. Y. Dzade, Prof. Dr. N. H. de Leeuw*
School of Chemistry, Cardiff University
Main Building, Park Place
CF10 3AT, Cardiff (United Kingdom)
[c] *Y. Zhang, Prof. Dr. J. P. Hofmann*
Laboratory of Inorganic Materials Chemistry
Department of Chemical Engineering and Chemistry
Eindhoven University of Technology
P.O. Box 513, 5600 MB Eindhoven (The Netherlands)
[d] *Prof. Dr. J. P. Hofmann*
Surface Science Laboratory, Department of Materials and Earth Sciences
Technical University of Darmstadt
Otto-Berndt-Strasse 3, 64287 Darmstadt (Germany)
[e] *Prof. Dr. N. H. de Leeuw*
Faculty of Geosciences, Utrecht University
Princetonlaan 8 A, 3584 CB Utrecht (The Netherlands)
[f] *Prof. Dr. N. H. de Leeuw*
School of Chemistry, University of Leeds
LT2 9JT Leeds (United Kingdom)

Supporting information for this article is available on the WWW under https://doi.org/10.1002/cptc.202000259

© 2021 The Authors. ChemPhotoChem published by Wiley-VCH GmbH. This is an open access article under the terms of the Creative Commons Attribution License, which permits use, distribution and reproduction in any medium, provided the original work is properly cited.

© 2021 The Authors. ChemPhotoChem published by Wiley-VCH GmbH

resolution of lower than 1 ns and probe spectral range of 350–900 nm (see SI for details). The charge carrier dynamics were monitored after laser excitation at 355 nm, at which wavelength the steady-state absorption spectra were similar for the studied samples. The g-C_3N_4 used in this study was synthesized by a typical thermal condensation method using urea as the precursor,[11] followed by pyrolysis and phosphorization reactions to obtain Co- and/or P-modified samples[9] (Co/g-C_3N_4, P/g-C_3N_4 and CoP/g-C_3N_4). Relatively low Co loading of ca. 0.5 wt% was chosen to ensure high optical transparency and minimize the light absorption of the CoP/g-C_3N_4 sample. The structure was confirmed by XRD, UV-vis and TEM (EDX) (Figures S1–S4). X-ray photoelectron spectroscopy (XPS) (Figure 1) demonstrated that P interacted with N in P/g-C_3N_4 and cobalt existed as oxidized states in Co/g-C_3N_4, while a CoP compound was formed in the CoP/g-C_3N_4 sample, which was in accordance with the reported results.[9,12]

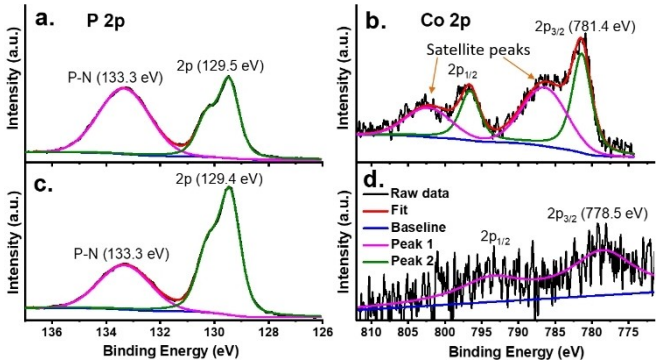

Figure 1. X-ray photoelectron spectroscopy (XPS) data of (a, c) P 2p and (b, d) Co 2p regions in (a) P/g-C_3N_4, (b) Co/g-C_3N_4 and (c, d) CoP/g-C_3N_4; the intensity of (d) was magnified by 1.5 fold to clearly show the peaks. The binding energy in the P 2p region around 133.3 eV corresponds to the interaction of P with N. The featured satellite peaks in the Co 2p region indicates the oxidized states of cobalt in Co/g-C_3N_4, and the oxidation state of CoP/g-C_3N_4 was similar to that of CoP structure.

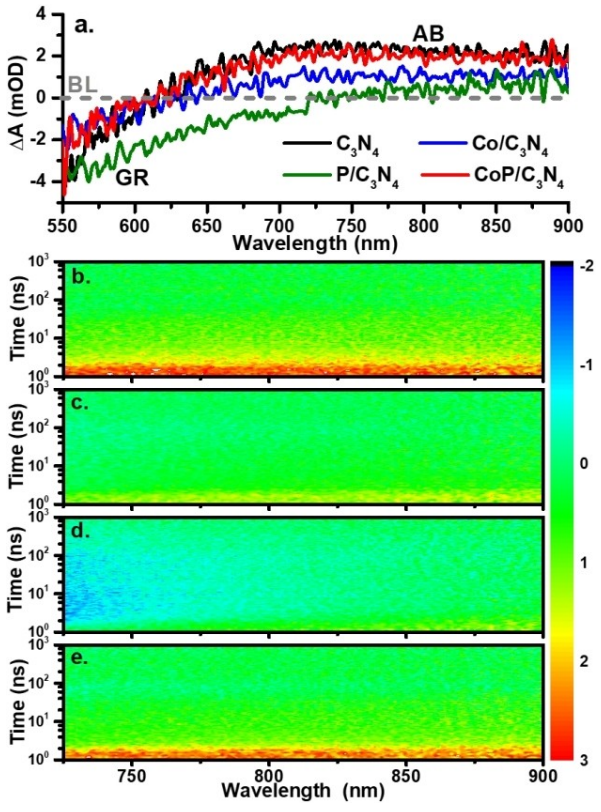

Figure 2. (a) Spectral slice taken from the transient absorption spectroscopy (TAS) data at the pump–probe time delay of 1 ns. The baseline (BL), ground state bleaching (GR) and photoinduced positive absorption (AB) were labelled. Hyperspectral TAS images are shown in (b) g-C_3N_4, (c) Co/g-C_3N_4, (d) P/g-C_3N_4 and (e) CoP/g-C_3N_4, after excitation with a pump laser pulse of 355 nm (2 μJ/pulse, 1000 Hz).

Figure 2a shows the TA spectral slice taken at a time delay of 1 ns for the synthesized samples in water. The spectrum of g-C_3N_4 was similar to that of Godin *et al.*,[8c] with the ground state bleaching around 550 nm and a positively broad absorption range above 600 nm. The positive absorption range has been ascribed to the photogenerated electrons,[8c,d] and was also confirmed by our TAS study, which showed that the broad absorption range was obviously enhanced when TEOA was added as the hole scavenger (Figure S5), while significant changes were observed in the TA spectra for the same g-C_3N_4 after Co or P modification. Co/g-C_3N_4 demonstrated lower positive absorption intensity, though with similar extended absorption range to that of g-C_3N_4. P/g-C_3N_4 displayed both lower positive absorption intensity and narrower absorption range, with the positive to negative crossover point of the TA spectrum moved to longer wavelength (~750 nm). However, the TA spectrum of CoP/g-C_3N_4 demonstrated obviously positive absorption in the compared range and displayed almost the same spectrum as that of g-C_3N_4 at the compared time slice of 1 ns.

The hyperspectral TAS images after 725 nm are shown in Figures 2b–e, which monitored the electron-induced TA spectra evolution. The broad photoexcited electron-induced hyperspectral image in Figure 2b indicates the long-lived electrons extended to long-timescale (μs) in g-C_3N_4. The absorption intensity was obviously lowered for Co/g-C_3N_4 (Figure 2c) and P/g-C_3N_4 (Figure 2d). In P/g-C_3N_4 in particular, the positive absorption at short wavelength changed to negative bleaching with prolonged time. CoP/g-C_3N_4 clearly displayed high photoexcited electron absorption intensity, while with prolonged time, the spectra evolution was obviously different from that of g-C_3N_4.

To elucidate the dynamics of photogenerated electrons, we monitored and compared the TA kinetics around 800 nm for all the samples. As shown in Figure 3a, following the same laser excitation intensity, g-C_3N_4 displayed high initial TA intensity, then showed a power law kinetic decay with a life-time longer than our spectral detection time limit (Figure S6a), which is due to the formation of photocatalytically inactive electron trap states,[8c,d] thus leading to low photoactivity. For Co/g-C_3N_4, the TA intensity decreased, which may be due to the decreased charge separation efficiency,[13] but it still displayed a life-time of up to microsecond timescale (Figure S6b). Compared with g-C_3N_4, an interesting phenomenon occurred for P/g-C_3N_4, which showed that not only did the TA intensity decrease, but

© 2021 The Authors. ChemPhotoChem published by Wiley-VCH GmbH

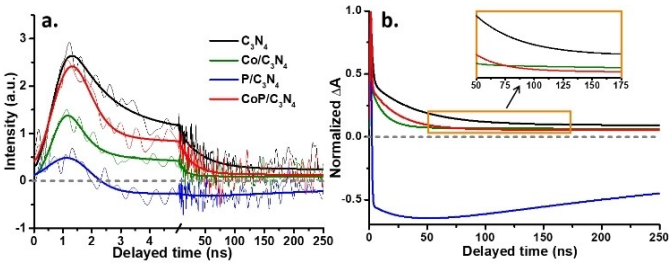

Figure 3. Transient absorption (TA) kinetic decays probed at 800 nm of g-C_3N_4, Co/g-C_3N_4, P/g-C_3N_4 and CoP/g-C_3N_4 in water after laser excitation at 355 nm (2 μJ/pulse, 1000 Hz): (a) before normalization, and (b) normalized fitting results with the inset shows the inverse phenomenon.

it also changed to a negative bleaching around 2 ns, with the bleaching extended outside of our spectral detection limit (Figure S6c), which may be ascribed to the trapping of photogenerated charges over P sites and will be discussed in the following section. After the formation of the CoP structure, CoP/g-C_3N_4 demonstrated completely different features compared to both Co/g-C_3N_4 and P/g-C_3N_4. The highest TA intensity of CoP/g-C_3N_4 only slightly decreased compared with that of pristine g-C_3N_4, while it demonstrated a different decreasing decay time around 3 ns, and with prolonged time the TA intensity was lower than that of pristine g-C_3N_4.

Furthermore, we use $t_{50\%}$ (the time at which the TA intensity of the photoexcited electrons has decreased by 50%)[13–14] to quantitatively compare the photogenerated electron dynamics. The $t_{50\%}$ of all the analyzed samples are in the order of g-C_3N_4 > CoP/g-C_3N_4 > Co/g-C_3N_4 > P/g-C_3N_4 (4.0, 2.8, 2.5 and 1.8 ns, respectively). Whereas Co and/or P modifications have been reported to exhibit higher photoactivity than pristine g-C_3N_4 for water splitting and CO_2 reduction,[5c–d,9] recent time-resolved spectroscopy studies have also shown that deeply trapped electrons with the life-time of longer than a microsecond were responsible for the limited H_2 evolution activity of g-C_3N_4;[8c,d] thus, the photocatalytic activity of g-C_3N_4 would be mainly affected by the photogenerated electron dynamics on the nanosecond timescale. The decreasing $t_{50\%}$ is an indication of promoted relaxation of photoexcited electrons in g-C_3N_4 after Co and/or P modifications. The transfer times of photoexcited electrons from g-C_3N_4 to Co and/or P are estimated to be 6.7, 4.9 and 3.3 ns for CoP/g-C_3N_4, Co/g-C_3N_4 and P/g-C_3N_4, respectively (see SI for calculation details). These results indicate that the promoted electron relaxation occurred on the timescale of several nanoseconds, and their capabilities to extract the photoexcited electrons from g-C_3N_4 were in an order of P/g-C_3N_4 > Co/g-C_3N_4 > CoP/g-C_3N_4. Furthermore, the weak signals of Co/g-C_3N_4 and P/g-C_3N_4 indicate the ultrafast quenching of the photogenerated electrons, which might be ascribed to the ultrafast bulk recombination of the electron-hole pairs, and thus may reduce the possibility of electron transfer to Co or P on picosecond timescales.

The normalized fitting results were compared in Figure 3b, where an inversed phenomenon around 75 ns (inset of Figure 3b) was observed between CoP/g-C_3N_4 and Co/g-C_3N_4. Such inversed phenomenon indicates that the electron trapping is less strong over CoP/g-C_3N_4, which may contribute to the higher photoactivity of the CoP co-catalyst rather than that of Co or P modification.[5c,9] This is also verified by the calculated work functions for Co/g-C_3N_4 and CoP/g-C_3N_4 which were 4.68 and 4.37 eV, respectively. With the lower work function for CoP/g-C_3N_4, the photoexcited electrons in CoP/g-C_3N_4 are more easily accessible for reactions, which may correspond to the inversed phenomenon of the spectra fitting results (inset of Figure 3b).

Further insight into the underpinning origins for the different TA kinetics was gained by DFT analysis. Compared with pristine g-C_3N_4 (Figure 4a), modification of the electronic band gap of the g-C_3N_4 was observed after Co and P doping, as shown in Figure 4b and c. Consistent with our XPS analysis and previous reports,[9,15] P was preferentially substituted at the C site (Figure 4c), whereas the Co was interstitially doped at the hollow site, bridging two N atoms (Figure 4b). The band gap of the pristine g-C_3N_4 was predicted at 2.80 eV, which was found to narrow upon Co (1.84 eV) and P (2.17 eV) doping. The valence band edge of the pristine g-C_3N_4 is dominated by N-*p* orbitals. Compared to P doping, the valence band edge is modified by Co doping, with the Co-*d* orbitals dominating the valence band edge of Co/g-C_3N_4. The average C–N distance in the pristine g-C_3N_4 is calculated at 1.335 Å, compared to a P–N

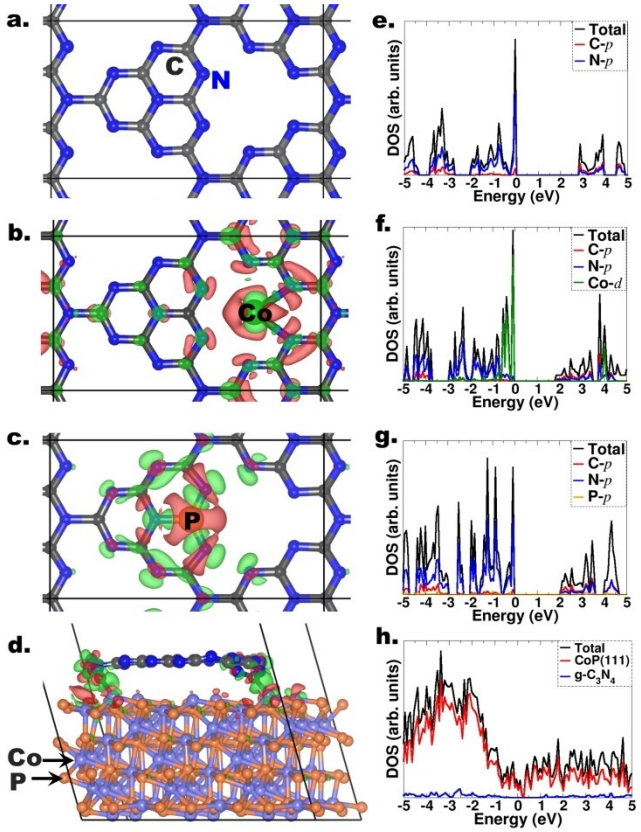

Figure 4. Optimized structures of (a) g-C_3N_4, (b) Co/C_3N_4, (c) P/C_3N_4 and (d) CoP(111)/C_3N_4, with their corresponding projected density of states (e)–(h). The green and red isosurface contours from different charge density analysis denote regions of charge density accumulation and depletion, respectively.

© 2021 The Authors. ChemPhotoChem published by Wiley-VCH GmbH

distance of 1.501 Å in the doped P/g-C_3N_4, whereas the average bridging Co–N bond distance in Co/g-C_3N_4 is predicted at 2.081 Å. The interface formation between g-C_3N_4 and the CoP (111) surface is found to induce a much larger reduction in the bandgap of g-C_3N_4, to 1.68 eV, which is consistent with the enhanced visible light absorption of the CoP/g-C_3N_4 sample (Figure S3). The significant reduction in the bandgap of g-C_3N_4 in the interface structure can be attributed to the intrinsic metallicity of bulk CoP (Figure S8) and its CoP(111) surface (Figure 4h).

The electron density redistribution and transfer between CoP and g-C_3N_4 was analyzed via differential charge density isosurfaces and Bader charge analyses. In the P/g-C_3N_4 system, the extra electron from the C substitution by a P atom delocalizes to the π-conjugated triazine ring, creating positively charged P^+ centers, which can promote efficient separation of photogenerated charges. Consistently, the calculated Bader charge of the P site ($+5.00\ e^-$) in P/g-C_3N_4 is higher than that of the interstitial Co sites ($+0.97\ e^-$) in Co/g-C_3N_4. The larger positive charge and thus stronger Lewis acid site of the P^+ centers indicates that the transfer of photogenerated electrons from g-C_3N_4 to P^+ would be much easier/faster than to the Co^+ centers, which is in accordance with the electron transfer time of our TA kinetic results (Figure 3). It has been verified that the photoexcited electrons will be produced by the N sites,[7a,9] and the XPS results in Figure 1a shows that there are strong P–N interactions in the P/g-C_3N_4 sample. Thus, the larger positive charge of the P^+ sites will also be responsible for the trapping of electrons to form catalytically inactive states, which induces the transition from a positive to a negative bleaching with prolonged time (Figure 3). Although P/g-C_3N_4 showed the fastest extraction of the photoexcited electrons in g-C_3N_4, the photoactivity is low due to electron trapping.[5c–d,9] It is evident from Figure 4d that electron density accumulates (green contours) around the centers of the newly formed C–Co bonds at the g-C_3N_4/CoP(111) interface, and Bader charge analysis demonstrates that the g-C_3N_4 loses about 0.67 electrons to the top of the CoP(111) surface, which may correspond to the relatively low capability to extract photogenerated electrons (Figure 3a). However, the work functions for g-C_3N_4, Co/g-C_3N_4, P/g-C_3N_4 and CoP/g-C_3N_4 were calculated at 4.88, 4.68, 4.59 and 4.37 eV, respectively. The lowest work function of CoP/g-C_3N_4 shows that the photoexcited electrons over CoP/g-C_3N_4 are more easily accessible for reactions.

In summary, the influence of Co and P on photoexcited electron dynamics in g-C_3N_4 is directly monitored on the nanosecond timescale, which is the timescale of the photoexcited electron transfer processes taking place in a g-C_3N_4 photocatalytic material. Combined with DFT calculations, further insights are provided for different electron relaxation processes, thus explaining the current reported results, which showed that a CoP co-catalyst displays excellent photocatalytic performance. The origin of this behavior may come from the promotion of photoexcited electron relaxation in g-C_3N_4 without significantly lowering the charge separation efficiency; these photoexcited electrons would be easily available for reactions. Furthermore, a special interface could form between CoP and g-C_3N_4 to enhance the visual light absorption and promote the photoexcited charge separation, which will also benefit the photocatalytic activity.

Acknowledgements

This work is part of the program "CO_2-neutral fuels" (project 13-CO26) of the Foundation for Fundamental Research on Matter (FOM), which was financially supported by the Netherlands Organization for Scientific Research (NWO). Additional support comes from the NWO Graduate Program "Solar Fuels Catalysis". Authors are also grateful to Petra Keijzer (Utrecht University, UU) for assistance with the TEM measurements, and Coen Mulder (UU) for performing ICP-AES measurements. NYD acknowledges the UK Engineering and Physical Sciences Research Council (EPSRC) for funding (Grant No. EP/S001395/1). This work has used the computational facilities of the Advanced Research Computing at Cardiff (ARCCA) Division, Cardiff University, and HPC Wales.

Conflict of Interest

The authors declare no conflict of interest.

Keywords: carbon nitride · cobalt phosphide · electron relaxation · photocatalysis · transient absorption spectroscopy

[1] a) Y. Tachibana, L. Vayssieres, R. J. Durrant, *Nat. Photonics* **2012**, *6*, 511–518; b) C. Jiang, S. J. A. Moniz, A. Wang, T. Zhang, J. Tang, *Chem. Soc. Rev.* **2017**, *46*, 4645–4660.

[2] a) R. Marschall, *Adv. Funct. Mater.* **2014**, *24*, 2421–2440; b) A. Kafizas, R. Godin, J. R. Durrant, *Semicond. Semimetals* **2017**, *97*, 3–46; c) P. Zhang, T. Wang, X. Chang, J. Gong, *Acc. Chem. Res.* **2016**, *49*, 911–921.

[3] a) X. Li, J. Yu, M. Jaroniec, X. Chen, *Chem. Rev.* **2019**, *119*, 3962–4179; b) J. Yang, D. Wang, H. Han, C. Li, *Acc. Chem. Res.* **2013**, *46*,1900–1909; c) K. Wu, H. Zhu, T. Lian, *Acc. Chem. Res.* **2015**, *48*, 851–859.

[4] a) P. Jiang, Q. Liu, Y. Liang, J. Tian, A. M. Asiri, X. Sun, *Angew. Chem. Int. Ed.* **2014**, *53*, 12855–12859; *Angew. Chem.* **2014**, *126*, 13069–13073; b) E. J. Popczun, C. G. Read, C. W. Roske, N. S. Lewis, R. E. Schaak, *Angew. Chem. Int. Ed.* **2014**, *53*, 5427–5430; *Angew. Chem.* **2014**, *126*, 5531–5534; c) Z. Huang, Z. Z. Chen, Z. Z. Chen, C. Lv, H. Meng, C. Zhang, *ACS Nano* **2014**, *8*, 8121–8129.

[5] a) D. K. Zhong, M. Cornuz, K. Sivula, M. Grätzel, D. R. Gamelin, *Energy Environ. Sci.* **2011**, *4*, 1759; b) P. Huang, J. Huang, S. A. Pantovich, A. D. Carl, T. G. Fenton, C. A. Caputo, R. L. Grimm, A. I. Frenkel, G. Li, *J. Am. Chem. Soc.* **2018**, *140*, 16042–16047; c) R. Shi, H.-F. Ye, F. Liang, Z. Wang, K. Li, Y. Weng, Z. Lin, W.-F. Fu, C.-M. Che, Y. Chen, *Adv. Mater.* 2018, 30, 1705941; d) Y. Zhang, T. Mori, J. Ye, M. Antonietti, *J. Am. Chem. Soc.* **2010**, 132, 6294–6295.

[6] a) M. Barroso, A. J. Cowan, S. R. Pendlebury, M. Grätzel, D. R. Klug, J. R. Durrant, *J. Am. Chem. Soc.* **2011**, *133*, 14868–14871; b) M. Barroso, C. A. Mesa, S. R. Pendlebury, A. J. Cowan, T. Hisatomi, K. Sivula, M. Grätzel, D. R. Klug, J. R. Durrant, *Proc. Natl. Acad. Sci. USA* **2012**, *109*, 15640–15645; c) Y. Ma, Andreas Kafizas, S. R. Pendlebury, F. L. Formal, J. R. Durrant, *Adv. Funct. Mater.* **2016**, *26*, 4951–4960.

[7] a) X. Wang, K. Maeda, A. Thomas, K. Takanabe, G. Xin, J. M. Carlsson, K. Domen, M. Antonietti, *Nat. Mater.* **2009**, *8*, 76–80; b) J. Liu, Y. Liu, N. Liu, Y. Han, X. Zhang, H. Huang, Y. Lifshitz, S-T. Lee, J. Zhong, Z. Kang, *Science* **2015**, *347*, 970–974; c) W.-J. Ong, L.-L. Tan, Y. H. Ng, S.-T. Yong, S.-P. Chai, *Chem. Rev.* **2016**, *116*, 7159–7329; d) M. Z. Rahman, C. B. Mullins, *Acc. Chem. Res.* **2019**, *52*, 248–257; e) F. Podjaski, J. Kröger, B. V. Lotsch, *Adv. Mater.* **2018**, 30, 1705477; f) V. W. Lau, I. Moudrakovski, T.

© 2021 The Authors. ChemPhotoChem published by Wiley-VCH GmbH

Botari, S. Weinberger, M. B. Mesch, V. Duppel, J. Senker, V. Blum, B. V. Lotsch, *Nat. Commun.* **2016**, *7*, 12165.
[8] a) C. Merschjann, S. Tschierlei, T. Tyborski, K. Kailasam, S. Orthmann, D. Hollmann, T. Schedel-Niedrig, A. Thomas, S. Lochbrunner, *Adv. Mater.* **2015**, *27*, 7993–7999; b) H. Zhang, Y. Chen, R. Lu, R. Li, A. Yu, *Phys. Chem. Chem. Phys.* **2016**, *18*, 14904–14910; c) R. Godin, Y. Wang, M. A. Zwijnenburg, J. Tang, J. R. Durrant, *J. Am. Chem. Soc.* **2017**, *139*, 5216–5224; d) K. L. Corp, C. W. Schlenker, *J. Am. Chem. Soc.* **2017**, *139*, 7904–7912; e) Z. Chen, Q. Zhang, Y. Luo, *Angew. Chem. Int. Ed.* **2018**, *57*, 5320–5324; *Angew. Chem.* **2018**, *130*, 5418–5422; f) M. A. Khan, P. Maity, M. Al-Oufi, I. K. Al-Howaish, H. Idriss, *J. Phys. Chem. C* **2018**, *122*, 16779–16787; g) L. Jing, R. Zhu, D. L. Phillips, J. C. Yu, *Adv. Funct. Mater.* **2017**, *27*, 1703484–9.
[9] W. Liu, L. Cao, W. Cheng, Y. Cao, X. Liu, W. Zhang, X. Mou, L. Jin, X. Zheng, W. Che, Q. Liu, T. Yao, S. Wei, *Angew. Chem. Int. Ed.* **2017**, *56*, 9312–9317; *Angew. Chem.* **2017**, *129*, 9440–9445.
[10] G. X. Pei, J. H. J. Wijten, B. M. Weckhuysen, *Phys. Chem. Chem. Phys.* **2018**, *20*, 9806–9811.
[11] D. J. Martin, K. Qiu, S. A. Shevlin, A. D. Handoko, X. Chen, Z. Guo, J. Tang, *Angew. Chem. Int. Ed.* **2014**, *53*, 9240–9245; *Angew. Chem.* **2014**, *126*, 9394–9399.
[12] a) H. Yang, J. Ouyang, A. Tang, *J. Phys. Chem. B* **2007**, *111*, 8006–8013; b) A. P. Grosvenor, S. D. Wik, R. G. Cavell, A. Mar, *Inorg. Chem.* **2005**, *44*, 8988–8998; c) Y. Zhang, L. Gao, E. J. M. Hensen, J. P. Hofmann, *ACS Energy Lett.* **2018**, *3*, 1360–1365.
[13] S. R. Pendlebury, A. J. Cowan, M. Barroso, K. Sivula, J. Ye, M. Grätzel, D. R. Klug, J. Tang, J. R. Durrant, *Energy Environ. Sci.* **2012**, *5*, 6304–6312.
[14] S. A. Haque, Y. Tachibana, D. R. Klug, J. R. Durrant, *J. Phys. Chem. B* **1998**, *102*, 1745–1749.
[15] J. Feng, D. Zhang, H. Zhou, M. Pi, X. Wang, S. Chen, *ACS Sustainable Chem. Eng.* **2018**, *6*, 6342–6349.

Manuscript received: October 30, 2020
Revised manuscript received: January 4, 2021
Accepted manuscript online: January 7, 2021
Version of record online: January 26, 2021

© 2021 The Authors. ChemPhotoChem published by Wiley-VCH GmbH